INTERNATIONAL ATOMIC ENERGY AGENCY
UNITED NATIONS EDUCATIONAL, SCIENTIFIC AND CULTURAL ORGANIZATION
INTERNATIONAL CENTRE FOR THEORETICAL PHYSICS
I.C.T.P., P.O. BOX 586, 34100 TRIESTE, ITALY, CABLE: CENTRATOM TRIESTE

SMR/534-6

ICTP/WMO WORKSHOP ON EXTRA-TROPICAL AND TROPICAL
LIMITED AREA MODELLING
22 October - 3 November1990

"A parametrization of orographic gravity wave drag. The impact of envelope orography and orographic gravity wave drag in the ECMWF model"

by

Tim Palmer

Presented by:
Prof. S. TIBALDI
Institute of Physics
Univ. of Bologna
Bologna, Italy

Please note: These are preliminary notes intended for internal distribution only.

Meteorological Training Course

Lecture Series

A parametrization of orographic gravity wave drag. The impact of envelope orography and orographic gravity wave drag in the ECMWF model

by

Tim Palmer

April 1987

European Centre for Medium-Range Weather Forecasts
Europäisches Zentrum für mittelfristige Wettervorhersage

A parametrization of orographic gravity wave drag. The impact of envelope orography and orographic gravity wave drag in the ECMWF model

In this lecture we shall discuss a simple parametrization of gravity wave drag, and study its effect in a series of integrations of the T42 ECMWF model. Much of the following is taken from Palmer et al. (1986) and Miller and Palmer (1987).

It is apparent from even the simplest linear theories of stationary, orographically forced gravity waves (see lecture Theory of linear gravity waves) that the character of flow over hills/mountains is sensitive to specific details of the upstream horizontal wind profile. Numerical studies of larger amplitude waves generated in more extreme circumstances suggest such a richness of dynamical behaviour and sensitivity to detail that parametrization of the dominant transport processes would seem to be out of the question. On the other hand, observational studies such as that of Brown (1983) indicate that under less extreme circumstances linear theory, judiciously interpreted, might form a useful basis for a parametrization scheme. Clearly, in devising a parametrization scheme we are not merely trying to mimic the momentum flux predicted by any specific theoretical model or measured in an observational study. The task is to represent the vertical flux of momentum due to subgrid-scale gravity waves by a parametrization scheme whose plausibility with respect to theory, observations and beneficial impact (in the GCM) are all maximized, though with economy of representation and computational efficiency paramount considerations.

There are two parts to the parametrization scheme used here: first a formula for the surface pressure drag exerted on the subgrid-scale orography and second a separate computation of the vertical distribution of wave stress accompanying the surface value.

Using Eq. (13) of the lecture "Theory of linear gravity waves", we present the surface drag by the expression

$$\underset{\sim}{\tau}_s = \kappa \rho N \underset{\sim}{u} . VAR \qquad (1)$$

where ρ and u are evaluated on the lowest σ level, and N is evaluated by a finite difference formula using values of T on the lowest two levels. The quantity VAR is equal to the variance of the subgrid-scale orography, as

determined by an orographic dataset (USA Navy) with a resolution of ten minutes of arc. The constant κ is regarded as a legitimately 'tunable' parameter, constrained only to an order of magnitude by linear theory. We have chosen a value of $2.5\times10^{-5}m^{-1}$, which (see lecture "Theory of linear gravity waves") gives reasonable values for the surface stress in our GCM integrations. This corresponds in linear theory to a horizontal wavelength of 250 km if the orographic variance is supposed to be sinusoidal. Since the subgrid-scale orography corresponds to scales between 20 and 200 km it is clear that our tuning constant is smaller than that suggested by a direct application of linear theory.

Given the vertical profile of wind, potential temperature and density, the second part of the parametrization scheme predicts the vertical profile of wave stress τ as a function of height. The problem is formidable, apart from the principal difficulty associated with the modification of propagating gravity waves by small-scale turbulence in the breakdown phase, one is faced with the basic three-dimensionality of real gravity wave systems, transience, the turning of the wind with height, diabatic heating, internal reflection and numerous other fluid mechanical subtleties. It is doubtful whether a parametrization scheme could address all of these difficulties without being as computationally demanding as a numerical model of the motion system itself. We base our parametrization scheme for breaking gravity waves on the simple steady, two-dimensional model of stratified flow discussed in Section 2 and invoke a saturation hypothesis similar to that of Lindzen (1981) to determine the stress distribution.

First of all we assume that the stress, τ, at any level is parallel to the surface stress vector and can be written as

$$\tau = |\underset{\sim}{\tau}| = \kappa\rho N U\, \delta h^2 \qquad (2)$$

where U is the magnitude of the component of the wind vector u in the direction of the surface stress (i.e. $U = (\underset{\sim}{u}.\underset{\sim}{\tau}_s)/|\underset{\sim}{\tau}_s|$).

Secondly we combine Eqs. (14) and (15) of the previous lecture (Theory of linear gravity waves), which describe the gravity wave's influence on static stability and vertical shear, to form a 'minimum Richardson number'

$$Ri_{min} = Ri\,\frac{1-(N\delta h/U)}{\left\{1+Ri^{\frac{1}{2}}(N\delta h/U)\right\}^2} \qquad (3)$$

which represents the smallest value the total Richardson number can achieve under the influence of the gravity waves.

For a monochromatic wave, Eqs. (14) and (15) of the previous lecture show that regions of maximum vertical shear are $\pi/2$ out of phase with regions of minimum static stability. However, following the notion of parametrizing the effects of an ensemble of phase-incoherent subgrid-scale gravity waves, the phase difference between Eqs. (14) and (15) in defining the compact expression for Ri_{min} in Eq. (3) has been ignored.

The condition that instability occurs when $Ri_{min} \leq 1/4$ embodies a convective over-turning criterion (numerator of Eq. (3) becomes small) (Lindzen 1981), and a billow instability mechanism (denominator of Eq (3) becomes large) (Scorer 1978). Following Lindzen we will employ a 'saturation' hypothesis whereby the displacement amplitude δh, in regions where $Ri_{min} < 1/4$ is reset so that $Ri_{min} = 1/4$. One can, in principle, therefore determine the vertical distribution of τ within the region $Ri_{min} \leq 1/4$, using the saturation hypothesis. Outside these regions the stress must be independent of height.

Consider now the algorithm for applying the Richardson number scheme. First of all the surface stress τ_s, is calculated (at each gridpoint) using Eq. (1). The Richardson number Ri is then calculated at the next σ-layer boundary using values of u, v and T stored on the adjacent σ levels. Using $\tau = |\tau_s|$, the displacement amplitude δh is estimated from Eq. (2) (using the average value of U on the adjacent σ levels). This value of δh is then substituted into Eq. (3) and Ri_{min} calculated. If $Ri_{min} \geq 1/4$ then τ at the σ-layer boundary is set equal to τ_s. If $Ri_{min} < 1/4$ then Ri_{min} is put equal to 1/4 and the saturation value δh_{sat} calculated from Eq. (3). τ_{sat} is then estimated using Eq. (2), and τ becomes equal to τ_{sat} at the layer boundary.

The whole procedure is now repeated to estimate τ at the next layer boundary and so on until we reach the lower boundary of the top layer. A value $\tau=0$ is imposed at the upper boundary, implying that the waves must be dissipated at least somewhere in the atmosphere.

Hence the wave stress is known at each layer boundary and the wave-induced acceleration at the σ levels can thus be calculated from the vertical gradient of the stress.

When invoking the saturation hypothesis to calculate δh_{sat}, Eq. (3) with $Ri_{min} = 1/4$ is a quadratic in δh_{sat} whose solutions is given by

$$\epsilon = Ri^{-\frac{1}{2}}(1 + 2Ri^{\frac{1}{2}})\{2Ri^{1/4}(1 + 2Ri^{\frac{1}{2}})^{-\frac{1}{2}} - 1\} \qquad (4)$$

where

$$\epsilon = N\ \delta h_{sat}/U \qquad (5)$$

From Eqns. (2) and (5)

$$\tau_{sat} = \epsilon^2 \kappa \rho U^3/N \qquad (6)$$

and the strong dependence of τ_{sat} on U shows why wave breaking is strongly preferred in regions of weak flow. As we go up through the model layers the decrease in density begins to play an important role. Perhaps of secondary importance in determining preferred locations for wave breaking is the dependence of τ_{sat} on N and ϵ^2. The appearance of N in the denominator shows that the stronger the static stability of the flow, all other variables kept constant, the smaller the value of τ_{sat} and hence the more readily waves will break. This is consistent with Scorer's (1978) remark that it is tilting of highly stable layers as air flows across hilly terrain which leads to the turbulence experienced by aircraft and glider pilots, and also with observations of shearing instabilities on the oceanic thermocline (Woods, 1968; Phillips, 1966).

On the other hand τ_{sat} is directly dependent on ϵ^2, which decreases from zero for Ri = 1/4 through a value of 0.21 for Ri = 1 to an asymptotic limit of 0.69 for Ri >> 1. Since, from Eq. (3), purely convective instability requires ϵ=1, wave breaking more readily occurs in our scheme than in a convective overturning scheme, even in the limit of large Richardson number.

If we put some rough figures into Eq. (4) we find that if ϵ^2=0.5(Ri~10) and $N=2\times10^{-2}\ s^{-1}$ then, with $\kappa = 2.5\times10^{-5}\ m^{-1}$, a flux of 0.1 Nm^{-2} will saturate in the boundary layer (ρ=1 kg m^{-3}) if U is less than about 5 ms^{-1}, in the mid troposphere if U < 7 ms^{-1} and in the lower stratosphere (ρ=0.05 kg m^{-3}) if U <15 ms^{-1}. Climatologically, values of U~5 ms^{-1} in the boundary layer and U~5 ms^{-1} in the lower stratosphere are not unreasonable in mid-latitudes and both of these regions are preferred locations for wave breaking (Lindzen, 1985). On the other hand mid-tropospheric winds will generally be strong enough to inhibit wave breaking.

As mentioned above, we apply the scheme using only the component of the model wind in the direction of the surface stress (or wind). When this component approaches zero the Richardson number becomes very small so that the effect of the scheme will be to drive δh_{sat} to very small values and cause the stress to be absorbed. In this way the scheme represents critical-level absorption for stationary gravity waves though since the critical level invariably falls between two model levels it is necessary to enforce the condition τ=0 at all layer boundaries above the critical line (defined as the level at which the component of the wind in the direction of the surface stress vector changes sign).

In view of the sensitivity of the wave Richardson number to the magnitude of the undisturbed static stability and wind speed one must consider how the observed structure in the vertical profiles of these fields influences our interpretation of the parametrization of wave breaking. It has long been recognized from the analysis of radiosonde ascents that wind, temperature and humidity do not vary smoothly with height but exhibit layers of radically different wind shear, static stability and dryness (Danielsen, 1959). Using raw radiosonde data, Danielsen plots vertical sections of observed potential temperature which show numerous shallow, highly stable layers sandwiched between layers of virtually neutral stability with horizontal continuity on the scale of thousands of kilometres. A variety of physical processes can contribute to the formation of a laminated vertical profile, such as the subduction of tongues of stratospheric air, frontogenesis, local mixing, cloud top radiational cooling and even inertia-gravity waves themselves. The question that needs to be asked is, 'What happens when a vertically propagating gravity wave passes through a highly variable vertical profile of wind and static stability?' It is clear from the Richardson number scheme that the waves are likely to break in the thin stable layers, yet they are also likely to break in the nearly neutral intervening layers if the

undisturbed Richardson number is less than 1/4. However, if a vertically smoothed profile is taken then the parametrization scheme might imply no breaking at all. One can immediately appreciate that breaking could be taking place to a much greater extent than suggested by a too literal interpretation of the monochromatic theory of wave breaking.

The major contribution to the wave stress given by Eq. (1) is the orographic variance and if VAR is simply the variance for a gridsquare then the wave stress is independent of wind direction (other than through directional correlations of N and $\underset{\sim}{V}_B$). This is an over-simplification since orography on most scales is highly anisotropic with pronounced nearly parallel ridges etc. To account for this basic effect, the subgrid scale variance was computed as four directional components (E/W, N/S, NW/SE, NE/SW). Fig. 1 gives examples of these directional variances. Flow parallel to major mountain ranges or plateaux no longer gives large wave stresses. The major ranges nevertheless present large variances to the incident flow, and typically these mountains act as a barrier to the flow, not necessarily as major gravity wave sources. Consequently the variance fields are reduced using simple dynamical criteria. The present operational scheme uses the relation

$$\text{VAR}_{\text{effective}} = \text{MIN}\ (\text{VAR}, \text{VAR}_{\tilde{R}})$$

where $\text{VAR}_{\tilde{R}}$ is the solution of Eq. (3) for δh^2 with Ri=1/4.

We shall conclude this lecture by studying the impact of envelope orography and gravity wave drag on a set of 90-day T42 wintertime integrations of the ECMWF model. These integrations were initialised using data from 6 December 1983, and had climatologically varying SSTs.

However, before showing results from these integrations it is worth considering the effect of a simple change to the boundary layer scheme. We have argued that C_{land} may be too weak. Why not just increase land surface roughness lengths? Fig. 2b shows the effect of a doubling of the surface roughness length in a 90-day T42 run. Compared to the control (Fig. 2a) we can see that there is little impact on the basic simulation of the large-scale flow.

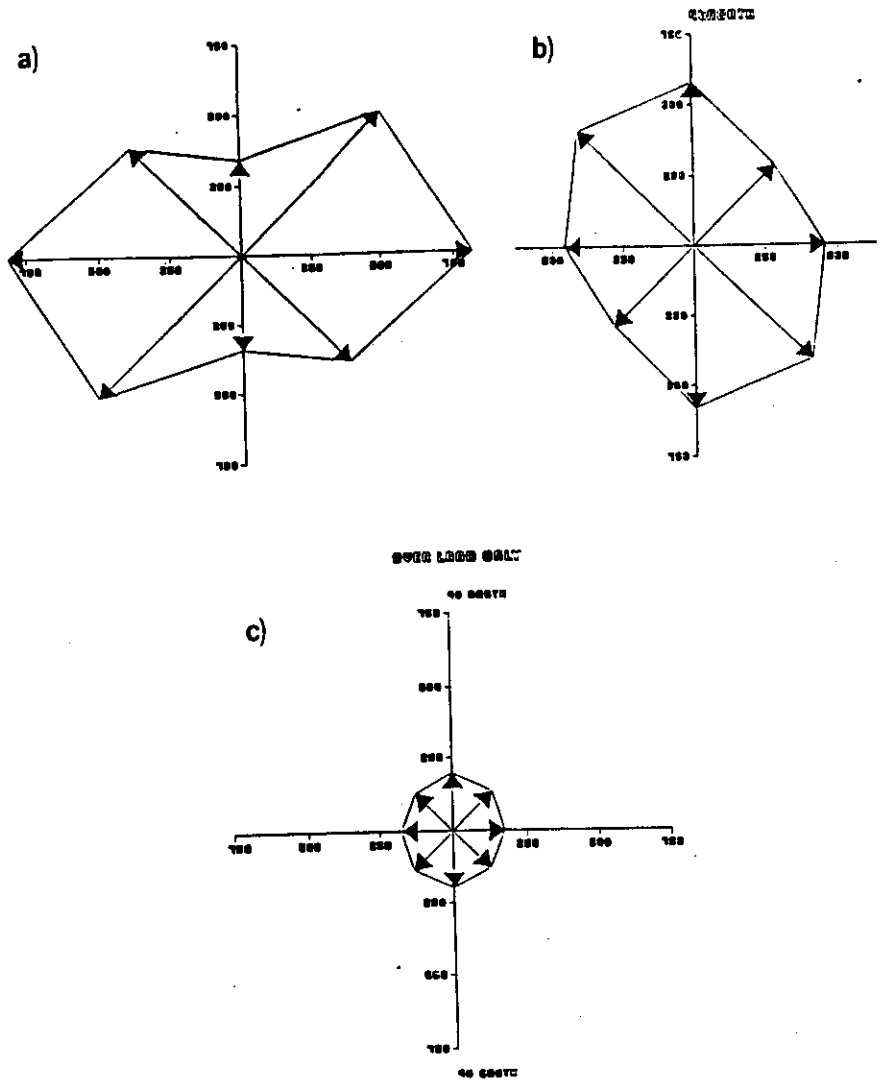

Fig. 1 The four components of subgridscale orographic standard deviation (in metres) for part of a) the Andes, b) the Alps, c) the Globe.

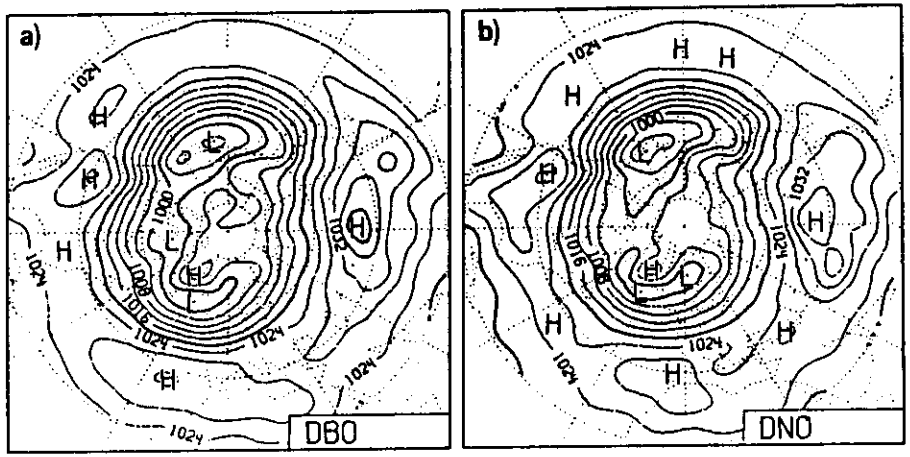

Fig. 2 Mean Northern Hemisphere surface pressure (mb) from 90-day wintertime integrations of the ECMWF T42 model with mean orography and
a) operational values for surface roughness lengths
b) doubled surface roughness length for momentum transfer

Perhaps, on reflection, one should not be surprised about this. Conventional boundary layer friction parametrizations attempt to describe the pressure drag associated with flow separation, and turbulent dissipation in the wake of small-scale roughness elements. Since stability will tend to suppress such flow separation, and the subsequent vertical diffusion of momentum in the turbulent wake, one can expect the flow to be largely insensitive to roughness length under stable conditions. Fig. 3, for example, shows the drag coefficient, for momentum, for the ECMWF model, in terms of the Richardson number, Ri. The coefficient is some ten times larger when Ri=1 than when Ri=+1.

Figs. 4-6 show 1000 mb time-mean and standard deviation of height, band pass and low pass filtered for integrations with mean orography only, ($\sqrt{2}\sigma$) envelope orography only, and envelope orography and gravity wave drag. Climatological values are also shown.

(The climatological data is taken from Lau et al., 1981. The band pass and low pass filters are those defined by Blackmon, 1976 and are used to define storm-track activity, and lower-frequency 'blocking' activity respectively. For the integrations, the time-mean height is calculated using all 90 days, and the filtered standard deviations are calculated by spectrally analysing the last 60 days of each integration, with band and low-pass filters equivalent to those used on the observations).

For the time mean fields, we can see that envelope orography by itself has made some improvement to the excessive westerly flow, though it is still too strong over the USA. Furthermore, there are unrealistically persistent anticyclonic conditions over Europe with strong surface winds displaced north Adding gravity wave drag to the envelope improves the time mean climate quite substantially, with no circumpolar isopleths in the time-mean 1000 mb height.

Similar improvements can be found studying variability within the integrations. With mean orography, the band-pass filtered standard deviation of 1000 mb height shows not only excessively strong storm tracks across most of the hemisphere, but also quite incorrect positioning of maximum and minim cyclonic activity (Fig. 5a). With envelope orography only storm track activity is also too intense over the landmases, and generally positioned to

far north. The observed maxima over the eastern seabords are not simulated (Fig. 5b). When gravity wave drag is added to envelope orography, the storm tracks are correctly positioned (Fig. 5c), with maxima over the western part of the Pacific and Atlantic oceans.

Finally, with mean orography only, low-frequency variability also appears to suffer, with no clear maximum over the west Atlantic (Fig. 6a). With envelope orography maximum low-frequency variability is positioned near the end of the storm track over the northern USSR, and the observed maximum over the west Atlantic is not simulated (Fig. 6b). Adding gravity wave drag to the envelope (Fig. 6c), low-frequency variability is well simulated with maxima of the correct magnitude just to the west of the British Isles and near the Aleutian Islands.

Of course, to base these conclusions on just one set of 90-day integrations would be somewhat unreliable, particularly for estimates of low-frequency variability. However, a set of multi-annual cycle integrations of the Meteorological Office GCM, with 2.5 x 3.75° latitude/longitude grid, has been made with mean orography, envelope orography, and mean orography plus gravity-wave drag. Some results from these integrations are described in Slingo and Pearson (1986). Fig. 7 illustrates the time-mean surface pressure over four winters of integration, with mean orography plus gravity wave drag. The northern hemispheric field is comparable to that shown in Fig. 1 of the lecture on resolution effects on systematic error. However, unlike its lower resolution counterpart, the model simulated the strength of the surface southern hemisphere westerlies fairly well. Fig. 8 shows standard deviation of monthly mean surface pressure from twelve winter months of an integration with mean orography only, and of the integration with mean orography and gravity wave drag. Values have been latitudinally averaged from 90N to 30N. It can be seen immediately that the major difference between the two curves is almost twice as much monthly-mean standard deviation as the run without. An observational estimate is also shown for comparison purposes.

The current operational model at ECMWF has both a 1σ envelope and a parametrization of gravity wave drag. Results show (Miller and Palmer, 1987) that the most consistent improvement to forecast skill comes from an inclusion of both processes rather than any one alone.

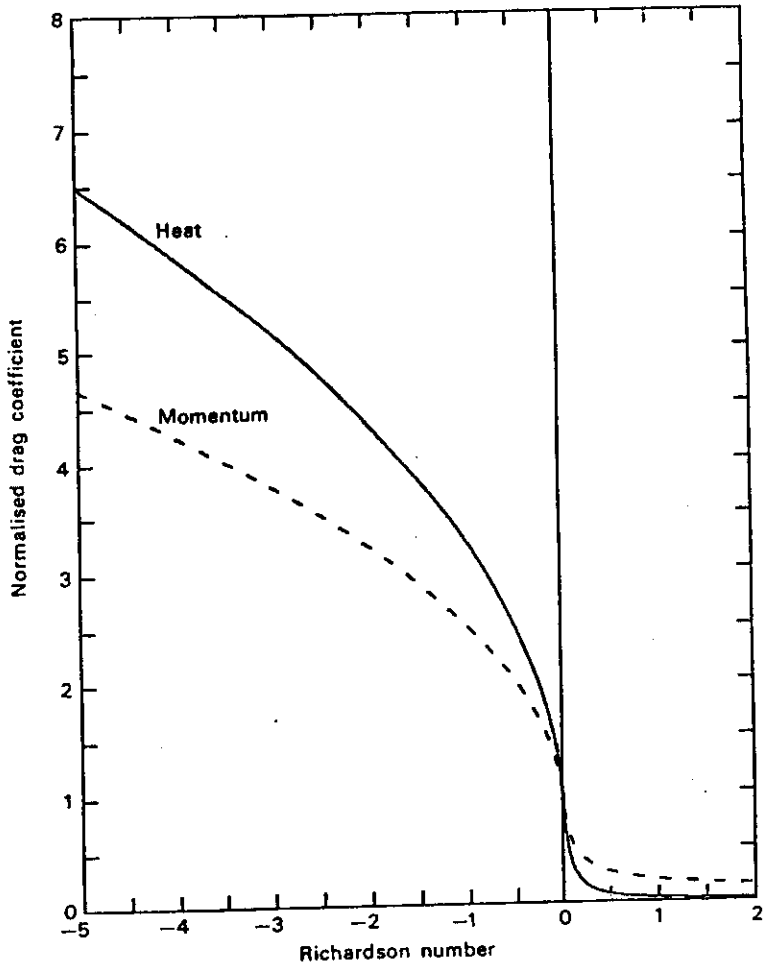

Fig. 3 Drag coefficients for heat and momentum as a function of Richardson number, in the ECMWF model.

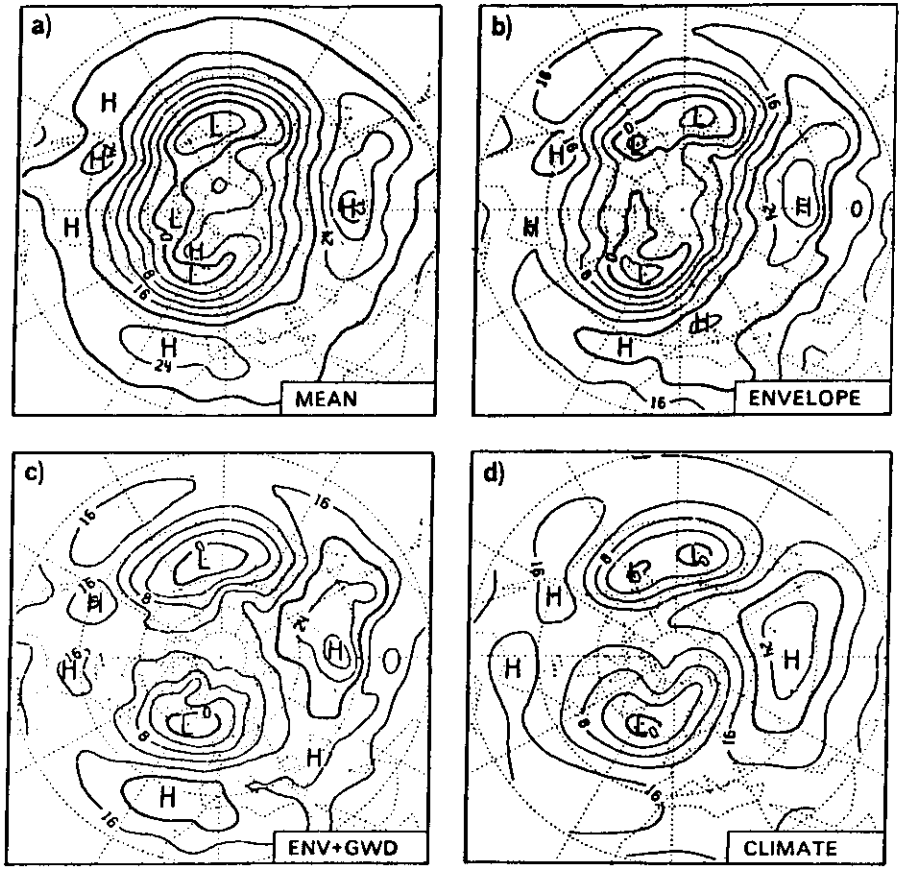

Fig. 4 1000 mb height (dam) averaged over a 90-day wintertime integration of the ECMWF T42 model. a) mean orography, b) envelope orography, c) envelope orography plus gravity-wave drag, d) observed climate. Contour interval 4 dam.

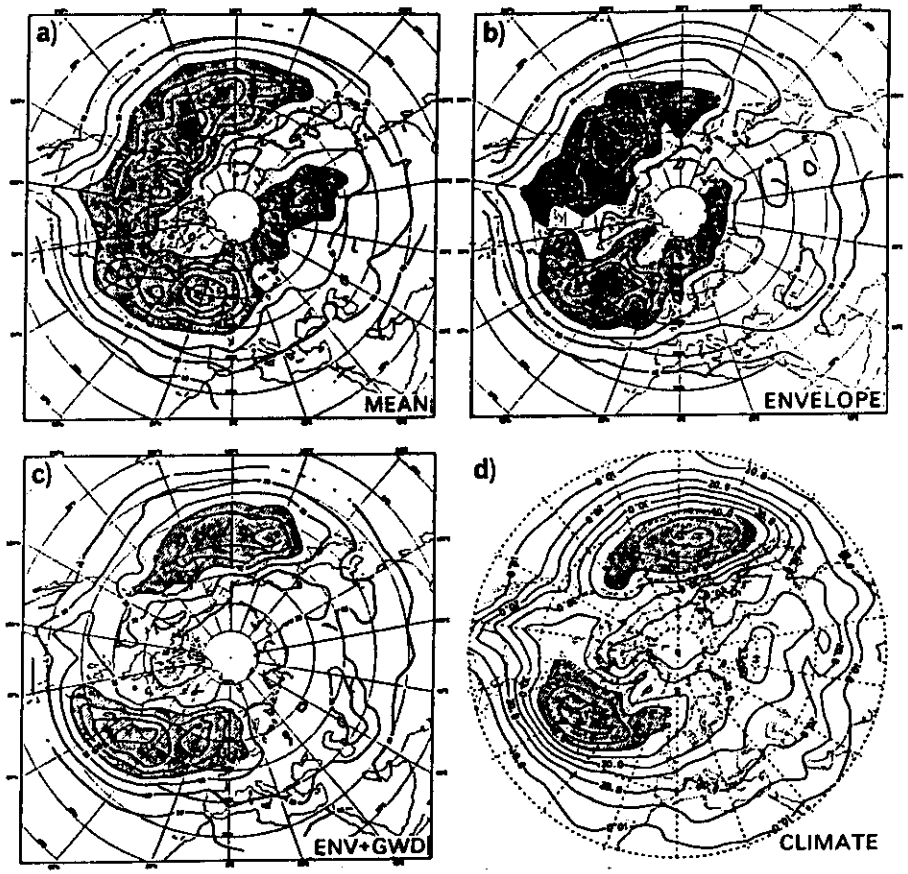

Fig. 5 As Fig. 4 but for band-pass standard deviation of 1000 mb height (m), calculated over last 60 days. Contour interval 10m in a), b) and c), and 5 m in d). Values greater than 40m are shown stippled.

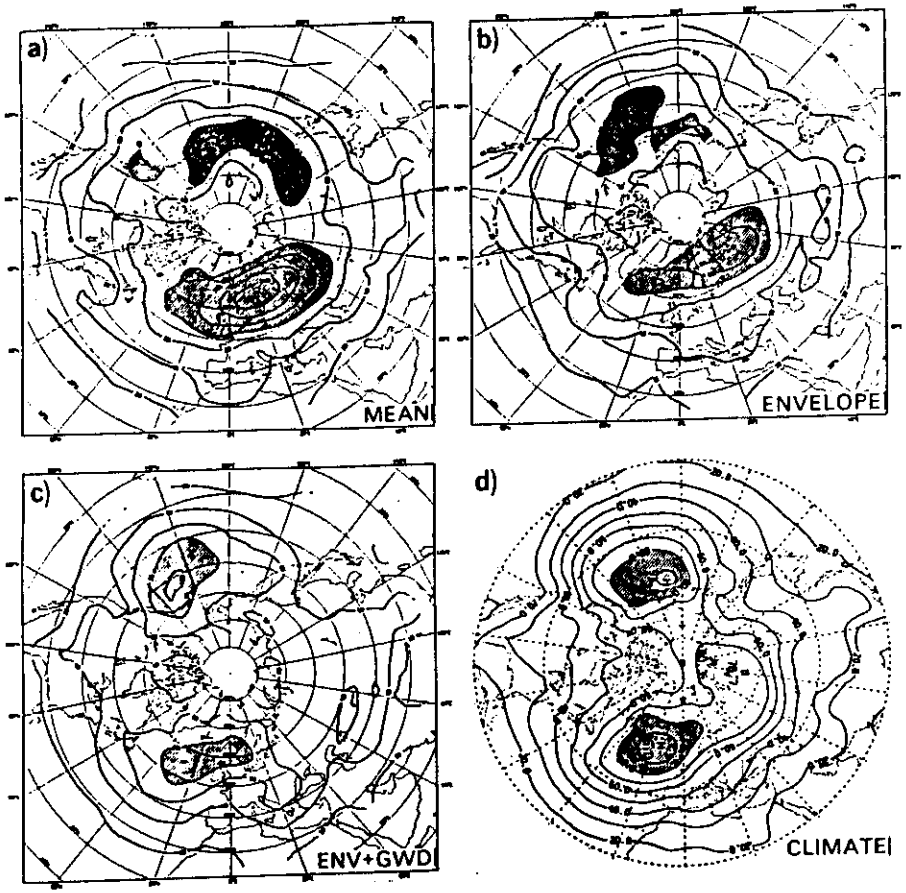

Fig. 6 As Fig. 4 but for low-pass filtered standard deviation of 1000 mb height (m), calculated over last 60 days. Contour interval 20m in a), b) and c), and 10m in d). Values greater than 80m are shown stippled.

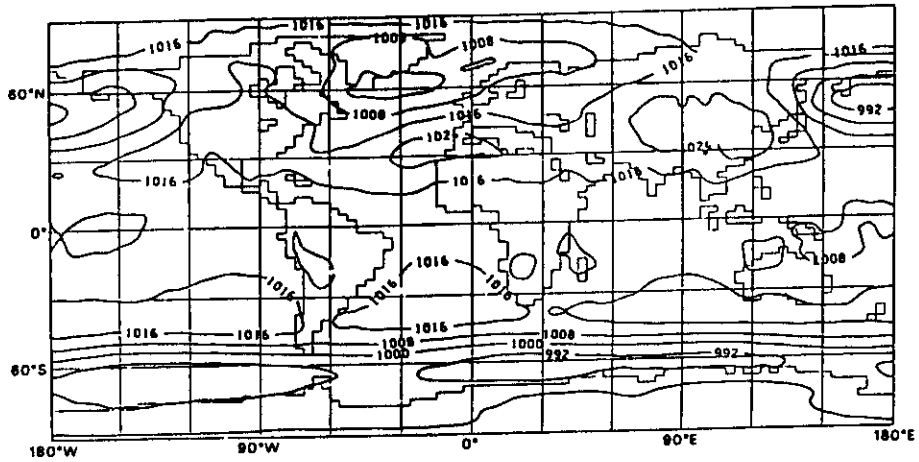

Fig. 7 Sea-level pressure (mb) for Dec-Feb for the mean of four winters from the Meteorological Office climate model with the gravity wave drag scheme. The contour interval is 8mb. From Slingo and Pearson, 1986.

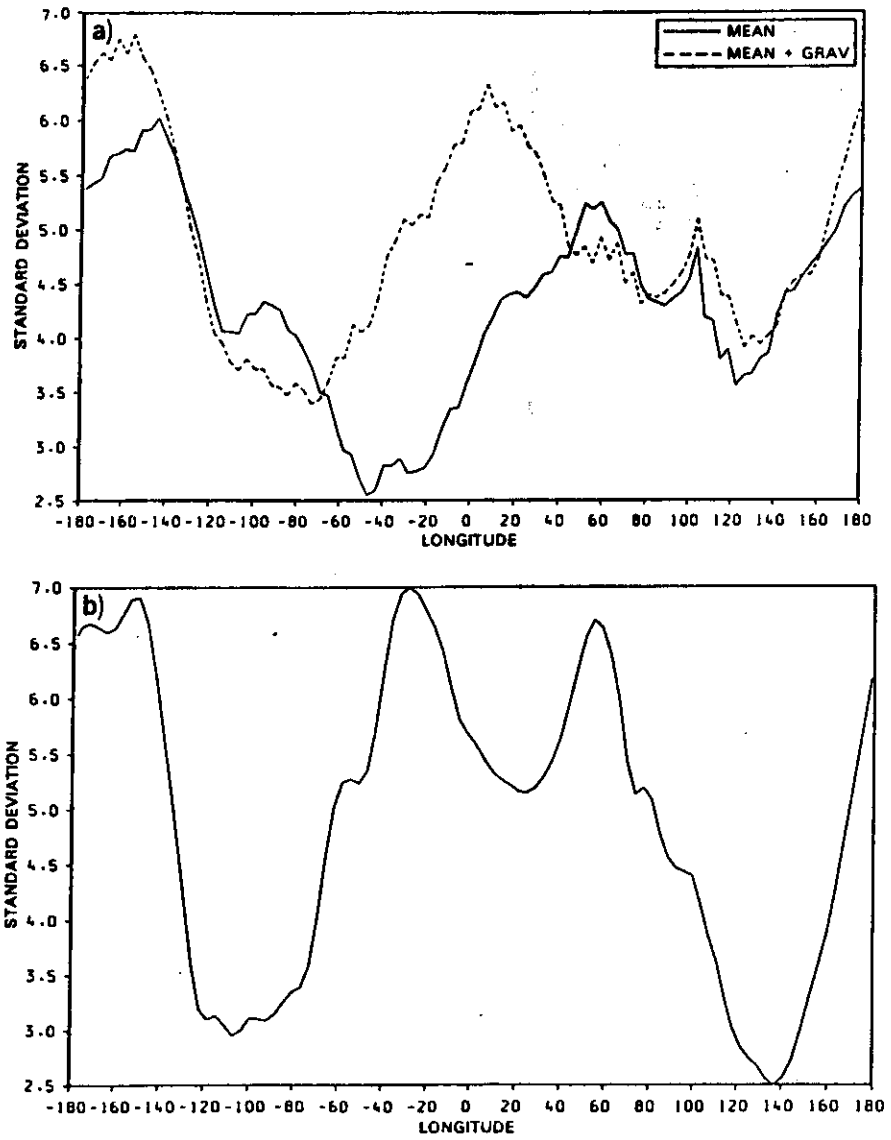

Fig. 8 Standard deviation of monthly-mean surface pressure (mb) a) from four year integrations of the Meteorological Office climate with mean orography, and with mean orography plus gravity wave drag. b) from three years of Meteorological Office archived data. Values have been latitudinally averaged between 30N and 90N.

References

Blackmon, M.L., 1976: A climatological spectral study of the 500 mb geopotential height of the northern hemisphere. J.Atmos.Sci., 33, 1607-1623.

Brown, P.R.A., 1983: Aircraft measurements of mountain waves and their associated flux over the British Isles. J.Atmos.Sci., 109, 849-866.

Danielsen, E.F., 1959: The laminar structure of the atmosphere and its relation to the concept of a tropopause. Arch.Met.Bioklim., 11, 293-332.

Lau, N.C., G.M. White and R.L. Jenne, 1981: Circulation statistics for the extratropical northern hemisphere, based on NMC analyses. NCAR Tech.Note. TN-171-STR, NCAR.

Lindzen, R.S., 1981: Turbulence and stress due to gravity wave and tidal breakdown. J.Geophys.Res., 86, 9707-9714.

Miller, M.J. and T.N. Palmer, 1987: Orographic gravity wave drag: its parametrization and influence in general circulation and numerical weather prediction models. ECMWF Seminar on Observation, Theory and Modelling of Orographic Effects, 15-19 September 1986. (Not yet published).

Palmer, T.N., G.J. Shutts and R. Swinbank, 1986: Alleviation of a systematic westerly bias in general circulation and numerical weather prediction models through an orographic gravity wave drag parametrization. Quart.J.Roy.Meteor.Soc., 112, 1001-1031.

Phillips, O.M., 1969: The dynamics of the upper ocean. Cambridge University Press, 261pp.

Scorer, R.S., 1978: Environmental Aerodynamics. Ellis Horwood Ltd., 488pp.

Slingo, A., and D.W. Pearson, 1987: A comparison of the impact of an envelope orography and of a parametrization of gravity-wave drag on simulations with an atmospheric general circulation model. Quart.J.R.Met.Soc., to appear.

Woods, J.D., 1968: Wave induced shear instability in the summer thermocline. J.Fluid Mech., 32, 791-800.